Anal. Bioanal. Electrochem., Vol. 16, No. 4, 2024, 315-330
https://www.doi.org/10.22034/abec.2024.712920

Analytical & Bioanalytical Electrochemistry

Full Paper

Electrochemical Direct Detection of Glycated Hemoglobin (HbA1c) by Immobilized Glucose Oxidase on ZnO Nanostructures

Javad Koohsorkhi,[1,2,*] Mehrshad Kafi,[1,2] and Sajjad Sanjari[1,2]

[1]*Department of MEMS and NEMS, School of Intelligent Systems, College of Interdisciplinary Science and Technology, University of Tehran, Tehran, Iran*
[2]*Advanced Micro and Nano Fabrication Devices Lab, University of Tehran, Tehran, Iran*

*Corresponding Author, Tel.: +98-9126771808
E-Mail: koohsorkhi@ut.ac.ir

Received: 25 September 2023 / Received in revised form: 25 April 2024 / Accepted: 26 April 2024 / Published online: 30 April 2024

Abstract- Electrochemical method is used for glycated hemoglobin (HbA1c) detection using a new configuration of working electrodes coated by ZnO nanorods. HbA1c reflects the average plasma glucose over two months. In this work, HbA1c is directly detected electrochemically without any proteolytic digestion for the first time. ZnO nanorods modify the working electrode to increase the surface of sensing, leading to amplifying the electrochemical signal and providing a stable enzyme bed for GOx immobilization. The limit of detection (LOD) is 0.32 µg/µl which can be achieved in 40 seconds as the sensor's response time. The range of detection is 0.32 µg/µl (0.21% of HbA1c)-22.4 µg/µl (14.93% of HbA1c) that covers the standard diagnosis range. Due to embedded nanostructures, a small amount of about 2 µl GOx solution and 50 nl of blood is required for detection. The low response time makes this sensor suitable for fast tests such as diabetic population enumeration and screening.

Keywords- HbA1c; Electrochemical; Glucose Oxidase; Zinc Oxide Nanostructures; Amperometry

1. INTRODUCTION

Diabetes mellitus is one of the most widespread disorders globally, with 422 million diabetic adults in 2014 [1], and this population increases annually, leading to 439 million by 2030 approximately [2]. Diabetes destroys the small veins in organs like the eye and kidney,

consequently causing complications such as Retinopathy, Nephropathy, Neuropathy, and Microalbuminuria [3]. Regular screening and early detection can prevent these disorders effectively. The 2009-released report of IEC (International Expert Committee), including members of ADA (American Diabetes Association), EASD (European Association for the Study of Diabetes), and IDF (International Diabetes Federation), concludes that HbA1c is the diagnostic marker of Diabetes. If HbA1c is above 6.5%, the patient will undoubtedly suffer diabetes [4]. HbA1c or glycated hemoglobin results from the attachment of glucose to the N-terminal valine of the hemoglobin, produced by glycating the amino acid of beta chains of hemoglobin molecules inside RBCs (Red Blood Cells) [5]. This marker determines the average of blood sugar in two months, and the examinee's real-time metabolic conditions do not affect the results, unlike plasma glucose, which needs special test conditioning. HbA1c observations help the patient to monitor the success of controlling diabetes programs in a period.

For the first time, in 1969, Rahbar demonstrated the correlation of Diabetes and HbA1c [6], and in 1976 Koenig suggested the regular measurements of HbA1c for monitoring the glucose metabolism [7]. Subsequently, several clinical methods have been developed like Liquid and Ion Exchange Chromatography, Electrophoresis, Spectrophotometry, Isoelectrofocusing, and immunoassay [8]. In 2002, the HbA1c standardization group and IFCC (International Federation of Clinical Chemistry and Laboratory Medicine) introduced the HPLC (High-Performance Liquid Chromatography) as the international reference method [9]. All these conventional techniques are time-consuming and need expensive equipment and trained experts. Therefore, research groups have developed inexpensive HbA1c electrochemical biosensors based on recognizing the protein's sugar moiety [10]. The electrochemical method has fair sensitivity and selectivity, and it is inexpensive, simple, and capable of miniaturization. Besides, nanostructures can be embedded to efficiently detect electrochemical signals due to their dimensions comparable with the analyte's small scale and raise the sensing component's surface-to-volume ratio.

There are two categories of electrochemical HbA1c sensors:

1- Direct detection of HbA1c

2- Indirect detection of HbA1c by determination of FV (Fructosyl Valine).

Furthermore, these biosensors' recognition components can be divided into three methods: Boronic acid derivatives, Antibodies, and Enzymes [10]. The first HbA1c electrochemical sensor was developed by Stollner in 2002, based on Haptoglobin and GOx-labeled anti-HbA1c antibody, and it was a direct detection [11]. Boronic acid HbA1c sensors were developed by modifying electrodes with ZrO_2 nanoparticles labeled by FcBA (Ferrocenboronic acid) [12,13], or gold electrodes modified by PBA (Poly amidoamine dendrimer bearing phenylboronic acid) [14,15], and in another work by electrodes with pTTBA/Au-NPs (poly terthiophene benzoic acid/Gold nanoparticles) [16]. Also, multi-mode integrated sensors of HbA1c, which can measure another biomarker such as hemoglobin or

plasma glucose in the same platform, are in demand and have been developed, despite the challenges of embedding different antibodies and enzymes in a single device [17]. For instance, voltammetry sensors have been built using PBA-PQQ (Pyrrolo Quinoline Quinone), covering electrodes with layers of phenylethylene on nanowires, with embedded Au nanoparticles labeled by Fc and modified by HbA1c antibody [8,18].

These sensors measure the HbA1c directly, but they need too much time to respond, e.g., three hours for Stollner's sensor. Some have a limited detection range and cannot cover the valuable diagnostic range of HbA1c (4%-7%). To overcome the mentioned challenges, indirect HbA1c sensors have been developed that benefit the enzyme properties [19-21]. In this approach, proteolytic digestion of HbA1c produces FV (Fructosyl Valine), and by FAOx (Fructosyl amino acid oxidase), FV is measured and results in the detection of the amount of HbA1c. FAOx as an enzyme has more sensitivity, selectivity, and response speed than boronic acid derivatives, and it is more stable and less expensive than the antibody. As one of the latest works on HbA1c biosensor, an amperometric biosensor has been fabricated with Au–Pt bimetallic nanoparticles and poly-indole-5-carboxylic acid-modified Au electrode. In this sensor, the FAOx enzyme was bio-conjugated onto a hybrid nanocomposite [21]. Though the advantage of these enzyme-based sensors, they need more complicated procedures to produce FV from proteolytic digestion of HbA1c, which means more cost and more time.

Our work proposes a direct enzyme-based HbA1c sensor. This research develops a new amperometric sensor with a modified gold working electrode by GOx (Glucose Oxidase) enzyme immobilized on ZnO nanorods. ZnO nanostructures have been used for glucose sensors widely [22-28], and in this work, they have been employed for HbA1c detection. Due to high surface area, biocompatibility, high-electron communicating features, and ease of syntheses, ZnO nanomaterials are recognized as superior candidates for electrochemical biosensors [29]. ZnO is also low-cost in comparison to other nanoparticles such as Au nanoparticles, and it does not have the toxicity of other nanomaterials like Au nanoparticles and Graphene [29]-[31].

Moreover, ZnO nanoparticles are chemo-resistive and are not susceptible to oxidative environments such as Graphene [29]. In this work, for the first time, ZnO structures are used for direct detection of HbA1c, though they have been used for indirect detections [32]. ZnO rods have been synthesized because ZnO's one-dimensional nanostructures represent more electrical conductivity than other structures [29]. Also, the GOx enzyme is used instead of antibodies due to its lower cost and more stability. This sensor responds to haemolysed real samples of RBCs just in 40 s, and it also covers the valuable diagnostic range. It needs 50 nl fresh whole blood and demonstrates high electrical currents in amperometry tests. The following includes preparing the sensor and samples, ZnO synthesis, and results, including CVs, SEMs, etc. Electrodes are designed with interdigits to enhance the rate of electron transformation. ZnO nanorods are used on top of the working electrode to improve the sensitivity of this sensor. GOx is used to activate the glucose of HbA1c in reduction and

oxidation cycles, as shown in Figure 1. Here, the GOx as an enzyme, affects the glucose bound to hemoglobin in the following oxidation & reduction reaction in order to the transfer of electrons between two reactants:

$$\text{Glucose} + O_2 \xrightarrow{GOx} \text{Gluconolactone} + H_2O_2$$

$$H_2O_2 \rightarrow O_2 + 2H^+ + 2e^-$$

Generally, hydrogen peroxide (H_2O_2), can act as both an oxidizing agent and a reducing. Therefore, the CV test was carried out in H_2O2. The glucose oxidase has been immobilized in ZnO nanorods on interdigits of the working electrode, which can be seen in Figure 1.

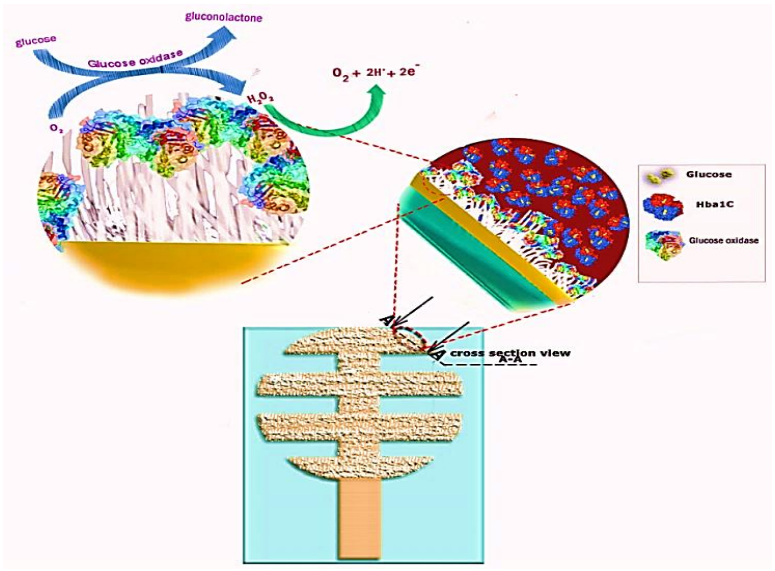

Figure 1. Reduction and Oxidation of glucose of HbA1c in the presence of GOx. GOx solution is immobilized in ZnO Nanorods, which are embedded on interdigits of the working electrode.

2. EXPERIMENTAL SECTION

2.1. Materials and methods

Chrome powder, Zinc nitrate tetrahydrate, HMTA (Hexamethylenetetramine), sodium acetate trihydrate, potassium hydroxide pellets, and acetic acid were purchased from Merck Germany. Ag/AgCl ink from ALS Company, Japan, Glucose Oxidase powder from Sigma-Aldrich, USA, Au target for DC sputtering, Shipley photoresist, gold and chrome etchant, and DI water were prepared too. Fresh Blood samples with measured HbA1c were provided by "Diabetes and Metabolic Diseases Clinic of Tehran".

Standard microfabrication processes were done by the instruments of the Advanced micro and Nano devices Lab., of the University of Tehran, including thermal evaporation and DC sputtering deposition, photolithography, and microinjection. MF 20-R centrifuge from AWEL France for sample preparation, ultrasonic bath for ZnO nanorods preparation, Dropsense

potentiostat (μStat 400) device for electrochemical measurements, and the HR-SEM apparatus of the 'Nanoelectronic and thin layer lab' of the University of Tehran for characterization of the sensor were used. All CV tests have been done in the Electrochemistry Institute of the University of Tehran.

2.2. Electrodes Fabrication

The transfer of electrons from all surfaces of the working electrode (side surface and top surface) occurs during oxidation and reduction reactions. In this article, for optimal design to increase the effective surface of the reaction, both surfaces are taken into consideration. To increase the side surface, the circular interdigit structure is used (Figure 2D), and to increase the upper surface, zinc oxide nanostructures are used.

Zinc nitrate hexahydrate ($Zn(NO_3)_2.6H_2O$), hexamethylenetetramine ($(CH_2)_6N_4$), polyethyleneimine (end-capped, molecular weight 800 g mol-1 LS), and tween 20 were all purchased from Sigma-Aldrich, and ammonium hydroxide(NH_4OH, 25%) was purchased from Merck. Human serum albumin (HSA) and anti-Human Serum Albumin antibody (HRP) (ab19183) were all purchased from Abcam. Phosphate buffer solution (PBS) and Tetra Methyl Benzidine (TMB) were all purchased from CMG. All solutions were made provision using deionized water**.**

Electrochemical experiments were performed by Source Meter instruments (Keithley 2602A). Two electrodes were used to measure current and voltage simultaneously, and the other was used as the working electrode. Morphological characteristics and crystalline structure of the samples were investigated using field-emission scanning electron microscope (Hitachi S-4160) (FESEM), and x-ray diffract meter using a PANalyticalX'Pert Pro MPD x-ray diffraction (XRD) with a Cu K-Alpha1 of 1.54060 A°. The data were analyzed by X'PertHighscore plus**.**

Microscope glass slides are cleaned and accurately prepared for gold electrode deposition. Since the gold layer cannot be deposited on glass firmly, an adhesion chrome layer with 30 nm thickness is deposited on slides by the thermal evaporation process. Afterward, a gold layer with 100 nm thickness is deposited by DC sputtering process. Each slide is cut in 11 mm as a USB port width, being ready for photolithography. The mask is designed based on USB electrode dimensions for providing stable output connections. The counter electrode (CE) has interdigits to enhance the electron transformations due to high electric fields on edges. The working electrode (WE) in the center is also designed with interdigits to keep and mix analyte, electrolyte, and enzyme properly. Figure 2D shows the mask and configuration of electrodes. The width and length of a USB electrode are 1.27 mm and 12.7 mm, respectively. The radius of WE is 1.5 mm with 500 μm width of each interdigit. The radius of CE is 3.8 mm, and its interdigits are 500 μm × 200 μm.

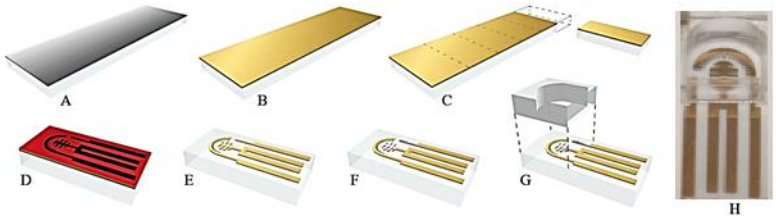

Figure 2. Sensor fabrication procedures, A) Chrome layer deposition B) Gold layer deposition C) Cut in USB dimensions D) Photoresist is spin-coated, and the mask is located E) Bare gold electrodes F) Deposit the Ag/Ag Cl ink on RE and ZnO on WE G) Plexiglas is attached as the chamber H) Photo of the fabricated sensor for inserting to USB interface.

After inspection of the fabricated electrodes' accuracy, they are washed by acetone and DI water and dried. Since the GOx enzyme's required buffer is quite acidic (in pH 5.0), gold electrodes are annealed in 540^{o}C for 15 minutes to obtain better adhesion and stability [33]. Ag/AgCl ink is pasted on the reference electrode precisely. Figure 2 demonstrates the fabrication steps of the sensor by the above standard processes. A clamp, including USB electrodes, is designed and built as the holder of the potentiostat test device's sensor and inputs for providing stable connections.

2.3. ZnO nanorods synthesis and deposition

We synthesized ZnO nanostructures using hydrothermal methods [34]. Aqueous solutions of 0.01 M zinc nitrate tetrahydrate and 0.01 M HMTA are prepared in 40 ml DI water and stirred for 10 mins. These combinations are optimal for producing the dense and uniform ZnO layers in the next steps. Glassy clean slides are located in prepared growth solutions, and ZnO rods grow on them after being in the oven for 5 hrs in 120^{o}C. Then, slides are extracted and ultrasonicated for 20 mins. Grown rods are detached from slides and float in DI water to obtain ZnO nanorods solution. These growth processes do not require a seeding phase because rods should be in solution form to deposit them on the working electrode. Now, rods need to be pasted on the interdigits of the working electrode precisely by utilizing the microinjection machine. Its syringe is filled with ZnO solution, and according to solution viscosity and 500 µm width of electrodes, the rate of injection and speed of syringe tip along the interdigits are entered into the system. After deposition, electrodes are located on the hotplate at 150^{o}C for water evaporation and better adhesion of rods on the working electrode. In another approach, for direct growth of ZnO nanostructures on the working electrode, a 5 mM solution of zinc acetate dihydrate in acetone is prepared and then spin-coated at 2000 rpm for 30 seconds to create a uniform Nano seed layer. Then, samples are heated in an ambient gas at 350°C for 20 mins to decompose the zinc acetate. A solution containing 25 mM zinc nitrate hexahydrate, 12.5 mM hexamethylenetetramine, 5 mM polyethyleneimine, and 0.8 M ammonium hydroxide in 200 ml DI water is prepared to grow ZnO nanostructures. To obtain thermal stability, this

process is carried out in the liquid bucket [35]. It is noteworthy to mention that there are other physical and green processes for ZnO nanorod synthesis, which can be more effective in mass-scale production [36-39].

2.4. Glucose oxidase immobilization

Initially, the powder of GOx is solved in the sodium acetate buffer. The 25 ml is obtained by solving 66 mg of sodium acetate trihydrate and 39.5 mg acetic acid in 25 ml DI water. Then, GOx is solved in buffer with 1 mg/ml solubility and stored at -20^{o} C. GOx solution is injected into ZnO rods of WE, and it is immobilized in the pores of rods.

2.5. Sensor integration

A Plexiglas frame is attached after preparing the electrodes, providing 200 µl total volume for decanting blood samples and electrolytes. First, three wires were connected to the sensor electrodes directly by Ag adhesive ink to provide the sensor's connections to an electrochemical analyzer device, but test results showed unstable and noisy response signals, as can be seen in Figure 3A.

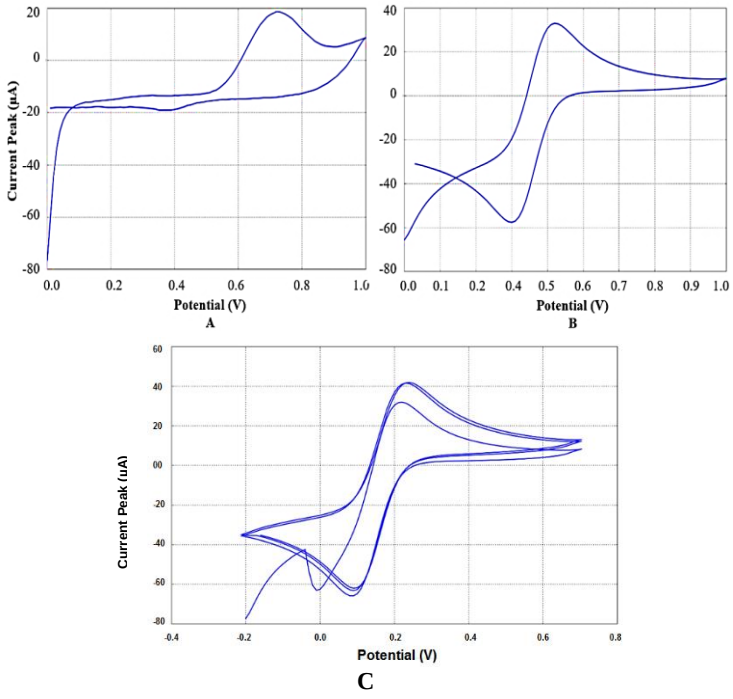

Figure 3. Electrodes performance: A) Noisy responses with Ag adhesive ink connections B) Stable and proper responses by USB clamp connections voltammograms at scan rate of 5mV/s for reference solution of reference solution 2.5 mM $[Fe(CN)_6]^{3-/4-}$ and C) Stability of responses through 3 continuous CV scans.

Consequently, a clamp with USB electrodes was designed, and it was attached to the sensor's electrodes to reduce the scratching gold electrodes and provide reliable connections. Then extracted wires of the clamp were connected to potentiostat inputs, and a new test was done, resulting in stable responses of Figure 3B.

Here, to investigate electrodes' proper operation, independent of the analyte and enzyme type, the reference solution, $[Fe(CN)6]^{3-/4-}$ was tested. USB prepares well-recognized CV responses leading to proper oxidation and reduction cycles. In forward at 0.22 V, the current peak is 33 µA, and in reverse at 0.10 V is -57 µA. Furthermore, there is no corrosion in gold electrodes due to adhesion layer deposition and annealing process, while the lack of them causes destroying electrodes after a few CV tests. In the next step, more scans were performed to observe the stability of the electrodes. As seen in Figure 3C, the voltammetry cycle was repeated three times continuously, and the appropriate reversibility of the electrodes and no change in efficiency in the cycles were obtained.

2.6. Preparing real hba1c samples

As the detection mechanism, the immobilized GOx activates each kind of glucose for acting in reduction and oxidation cycles shown in Figure 1, including the Glucose of the HbA1c. To achieve the biosensor's selectivity, whole blood components are separated initially to avoid the interference of any other kind of glucose in sensor response. Fresh blood is centrifuged by 3000 rpm for 5 minutes to make RBCs separated from plasma [40]. RBCs get settled down and are collected. They are haemolysed by adding DI water eight times more than their volume. The only glucose remaining in samples belongs to HbA1c, ready for putting them in the sensor, and the amperometry responses illustrate the HbA1c concentrations. A similar separation of HbA1c and measuring them by GOx has been reported [11,15].

3. RESULTS AND DISCUSSION

3.1. Characterizations of ZnO nanostructure

Figures 4A, B, and C demonstrate SEMs of ZnO nanorods synthesized for pasting on working electrode, and Figures 4D and E depict directed grown rods. Figure 4A shows the high porous and high dense ZnO layer, which is adequate for GOx immobilizing, electron transferring, and providing more sensitivity by raising the surface-to-volume ratio. Figures 4B and C, with more magnifications, illustrate nanorods' dimensions and their hexagonal structures. Figure 4D and E, showing the SEM images of the ZnO structures grown on the working electrode, indicating that the length of ZnO rods is 2 µm approximately.

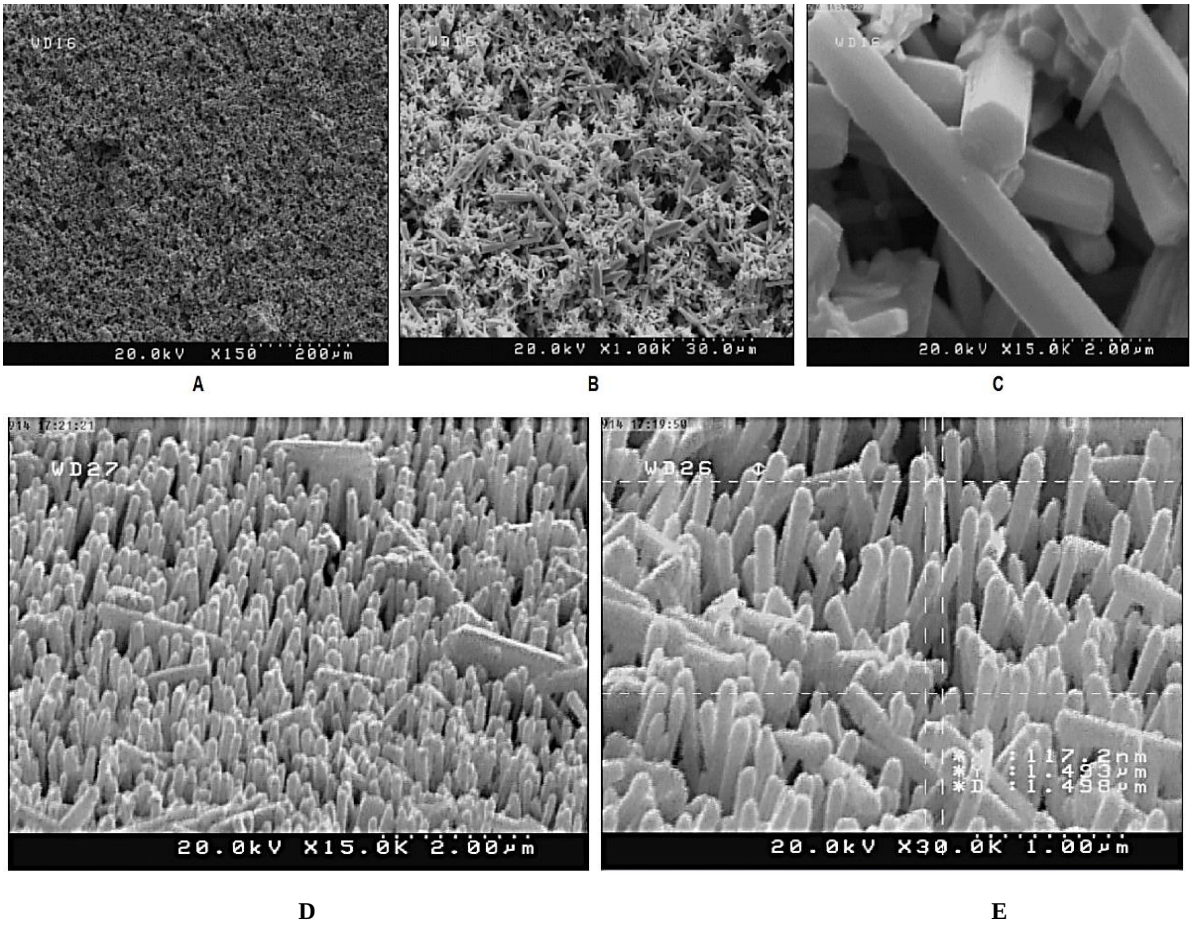

Figure 4. SEM images of synthesized ZnO Nanorods A) Uniform and high dense layer of ZnO rods, x150 magnification (scale of 200µm), B) Porosity of synthesized ZnO, x1.00K magnification (scale of 32.0µm), C) Hexagonal structure of Nanorods, x15.0K magnification (scale of 2.00µm), D) Synthesized ZnO Nanostructures using seed-based hydrothermal methods with uniform, high density, and aligned ZnO Nanostructure, x15.0K magnification (scale of 2.00µm), E) Length (17.2nm) and width (5nm) of rods, x30K magnification (scale of 1.00µm).

3.2. ZnO rods assessment

As mentioned at the beginning, ZnO nanostructures are effective due to increasing the effective surface of the reaction and also improving the electrode for the transport of electrons. For analysing ZnO rods' effect, two tests are carried out: First, a sensor with ZnO rods on the working electrode and then a sensor with a bare working electrode without ZnO rods are tested. Other conditions are the same. Figure 5 clears the difference: 20.1 µA current peak for the sensor without ZnO and 49.2 µA for ZnO embedded sensor are observed. It is evident that nanorods improve electron transfer more than two times, and consequently, the sensitivity becomes 2.45 times higher. The current in the modified sensor's peak is more precise and readable, increasing the sensor's resolution and magnifying the difference between amounts of HbA1c. On the other hand, ZnO nanorods' porous structures help to immobilize and

concentrate GOx on the working electrode efficiently and raise the analyte's interaction with the enzyme. Hence, 2 µl of GOx solution on the working electrode is enough to provide a current CV response peak.

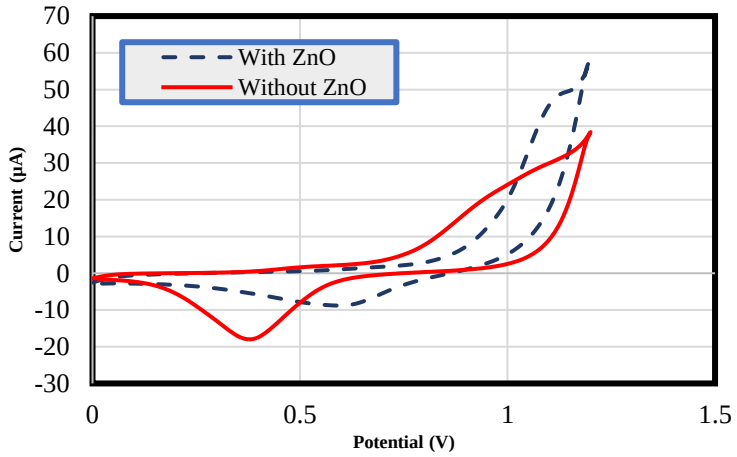

Figure 5. Comparison of sensors with ZnO and without ZnO: 20.1µA current peak for the sensor without ZnO and 49.2µA for ZnO embedded sensor

3.3. Optimization

Figure 6A demonstrates the results of CV tests with different scan rates to determine the sensor's optimized scan rate and, consequently, achieve the sensor's high response speed.

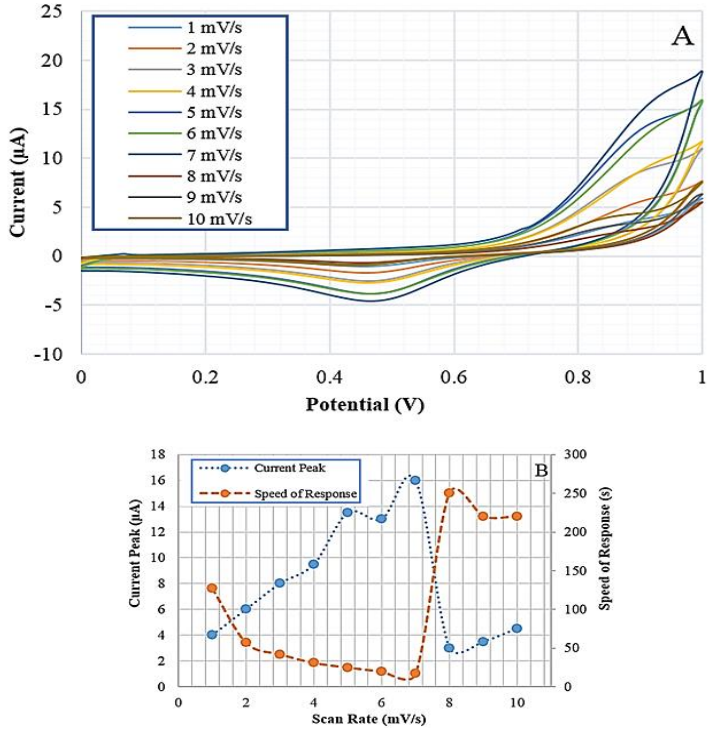

Figure 6. Optimal scan rate and speed of response of sensor A) Voltammograms at different scan rates. B) Current peaks and response times versus scan rates.

In these tests, 100 µl of haemolysed RBCs and 100 µl sodium acetate buffer as the electrolyte is used. Scan rates varied from 1 mV/s to 10 mV/s, and cycles are compared. The minimum and maximum potentials are set to 0 and 1 V, respectively, and no peaks are observed out of this area. According to observations of different scan rates, Figure 6B compares the peaks and response times, concluding that 7 mV/s has the highest current peak with 16 µA and has the minimum response time with 20 s for each complete cycle. Before 7 mV/s, the scan rate and speed of response are slower and do not provide sufficient potential for the full reaction of glucose of HbA1c, and as a result, the peak is lower**.** On the other hand, after 7 mV/s, the speed of potential scanning is too high, and therefore the time for the analyte's complete reaction is limited, and then lower electrons are exchanged, though electrodes reach sufficient potential. Usually, each amperometry test's second cycle has a more stable peak, so the sensor's response speed is estimated 40 s instead of 20 s. This response time makes the sensor suitable for point-of-care fast detection of HbA1c without considering blood samples' corruption.

3.4. Calibration

The sensor assesses samples with different concentrations of HbA1c with a scan rate of 7 mV/s. The volumes of samples are the same, and the only difference between them is their HbA1c concentrations, so the only reason for variations of peaks belongs to HbA1c concentrations. Figure 7 demonstrates the CV responses of them and displays the current peaks versus HbA1c concentrations.

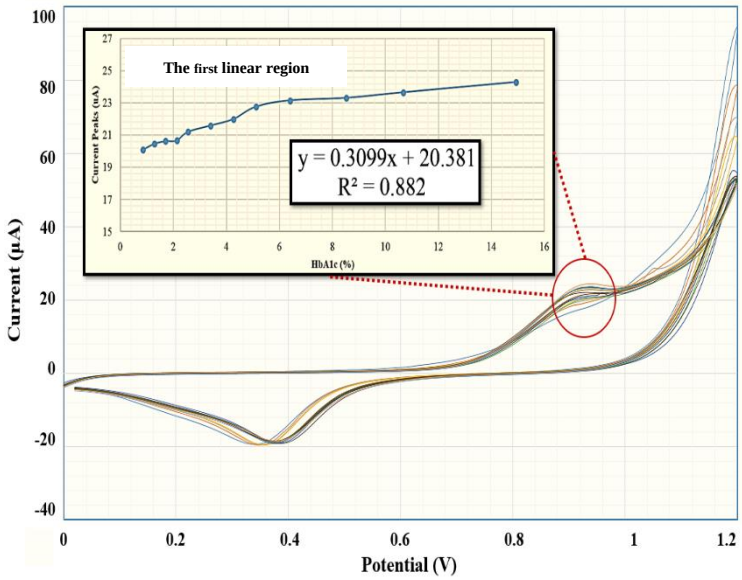

Figure 7. Different concentrations of HbA1c to calibrate the sensor

In Figure 7, the magnified graph shows the two linear regions with two different slopes, the slope of the first linear region is 0.31 µA/HbA1c% and can be fitted from 2.13% to 8.53% of

HbA1c covering the valuable clinical area. This sensor can measure HbA1c concentrations as low as 0.32 µg/µl equal to 0.21% of HbA1c until as large as 22.4 µg/µl equal to 14.93 HbA1c% before saturation. Therefore, the limit of detection of a sensor is 0.32 µg/µl, and the range of detection is 0.32 µg/µl-22.4 µg/µl. To investigate the sensor's accurate sensitivity, we gradually increase the concentration of the limit of detection (0.32 µg/µl), reading the output current peak in each enhancement simultaneously. The first apparent distinguishable peak is observed when the concentration becomes 0.64 µg/µl, which illustrates the sensitivity of 0.32 µg/µl. By adding 0.32 µg/µl, we can observe the next clear, readable current peak in each step. This resolution corresponds to 0.21% is in the order of the portable HbA1c devices in the marketplace, such as A1cNowInView™ [41].

In optimal CV parameters such as 0.0V-1.2 V and 7 mV/s, 100 CV scans are done continuously to assess responses' stability. As seen in Figure 8, peaks variation is 30.68 µA to 37.96 µA, and in the entire range of currents (-27.07 µA to 37.96 µA), there is an 11.19% response degradation in 100 scans. Without annealing the gold electrodes, after 1 minute of testing, the working electrode's gold gets scratched, destroyed, and disappeared, whereas, by annealing, it does not face any destruction even after 100 cycles that last about 40 minutes. The 11.19% degradation from the first fresh cycle can be interpreted as reducing the efficiency of GOx and the electron transferring ability of the buffer among electrodes. However, after 100 scans, the sensor still works, and the peaks can be observed.

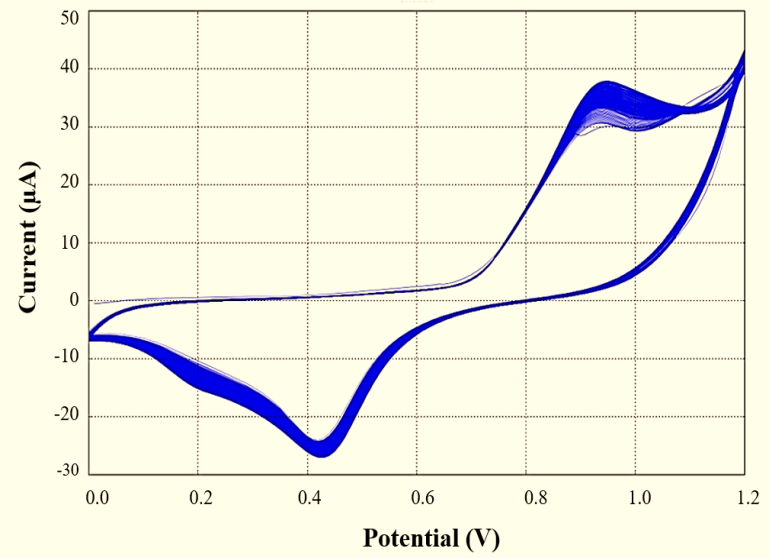

Figure 8. Stability of responses through 100 continuous CV scans. Peaks variations are 30.68 µA to 37.96 µA leading to 11.19% degradation

To compare with the other works, Table 1 indicates important parameters of HbA1c electrochemical detection sensor with similar studies. In these researches, like the proposed sensor, the direct method of measuring HbA1c has been adopted.

Table 1. Comparison of different research groups' outstanding similar sensors

Electrode/Interface Material	Mechanisms of Detection	Response time	Current Peak	Range of Detection	LOD	Ref.
ZnO Nanostructures/Au	Voltammetric	40 s	37.96µA	0.32-22.4µg/µl 0.21%-14.93%	0.32µg/µl 0.21%	This work
Membrane-immobilized haptoglobin as an affinity matrix	Amperometric and CV	3 hrs	150nA	5-20% 0.2-5µg/ml	5% 0.2µg/ml	[11]
Zirconium dioxide nanoparticle-modified pyrolytic graphite electrode (PGE)	Amperometric	30 mins	2µA	6.8%-14%	6.8%	[12]
Boronic acid-modified electrodes	Electrochemical detection	30 mins	3.25µA	2.5%-15%	2.5%	[14]
Boronate-modified electrode	Electrochemical detection	N/A	2.25µA	4.5%-15%	4.5%	[15]
pTTBA/AuNPs	Amperometric	20 mins	3.5µA	0.1%-1.5% 0.5%-6.0%	0.1%	[16]
ZnONPs/PPy/Au electrode	Amperometric and CV	25 s	25 µA	4%-12%	4%	[42]
Graphene oxide composites	Voltammetric	NA	NA	9.4%-65.8%	9.4%	[43]

As seen in Table 1, the previous fastest response was reported as 25 s [42], and the highest current peak was 25 µA [42], which are 40 s and 37.96 µA, respectively, for the proposed sensor in this article. Comparing the results of Table 1, it can be seen that the response time of the sensor and the blood needed to perform the test are optimal. Low blood volume and high speed make this sensor very suitable for diagnostic tests and rapid tests. Also, the maximum peak current at the highest HbA1c concentration of each has been compared. The relatively higher current peak of the proposed sensor makes a simpler read-out circuit and makes it easier circuit integration. In measurement range comparison, although it does not include the highest range than the others but the proposed sensor covers the entire range (i.e. from 4%-7% of HbA1c) with diagnostic value, diabetic population enumeration, and screening.

4. CONCLUSION

In this research, an electrochemical sensor for direct detection of HbA1c is designed and fabricated. Due to the design of working and counter electrodes and embedding ZnO nanorods on working electrodes, this sensor works with a fast response time of 40 s and a high current peak of 37.96 µA in comparison to other previous similar works (Table 1). Although the sensor does not have the most expansive detection area, it covers the valuable medical diagnostic area. Using the GOx enzyme instead of the HbA1c antibody, the sensor's cost becomes inexpensive comparably. Nevertheless, it needs the plasma separation process, and as future work, by

integrating a plasma glucose sensor with this sensor, this step can be omitted with differential processing leading to a dual-mode sensor with just one enzyme in one platform.

Acknowledgments

Sincere gratitude is hereby given to Dr. Hosseini for providing us with the test equipment at the Electrochemistry Institute of the University of Tehran and Ms. Forouzanfar provided us with the fresh blood samples from the Diabetes Metabolic Diseases Clinic of Tehran.

Declarations of interest

The authors declare no conflict of interest in this reported work.

REFERENCES

[1] World Health Organization, Global Report on Diabetes, WHO Library Cataloguing in Publication Data (2016).
[2] J.E. Shaw, R.A. Sicree, and P.Z. Zimmet, Diabetes Res Clin Pract. 87 (2010) 4.
[3] B.K. Tripathi, and A.K. Srivastava, Med. Sci. Monit. 12 (2006) 130.
[4] The International Expert Committee, Diabetes Care (2009)
[5] D.B. Sacks, Carbohydrates, Elsevier Saunders (2006).
[6] S. Rahbar, O. Blumenfeld, and H.M. Ranney, Biochem Biophys. Res. Commun. 36 (1969) 838.
[7] R.J. Koenig, C.M. Peterson, R.L. Jones, C. Saudek, M. Lehrman, and A. Cerami, N. Engl. J. Med. 295 (1976) 417.
[8] B. Wang, Materials 8 (2015) 1187.
[9] J.O. Jeppsson, U. Kobold, J. Barr, A. Finke, W. Hoelzel, T. Hoshino, K. Miedema, A. Mosca, P. Mauri, R. Paroni, L. Thienpont, M. Umemoto, and C. Weykamp, Clinical Chemistry and Laboratory Medicine (CCLM) 40 (2002) 1.
[10] H. Lin, and J. Yi, Sensors 17 (2017) 1798.
[11] D. Stöllner, W. Stöcklein, F. Scheller, and A. Warsinke, Anal. Chim. Acta 470 (2002) 111.
[12] S. Liu, U. Wollenberger, M. Katterle, and F.W. Scheller, Sens. Actuators B 113 (2006) 623.
[13] J. Halámek, U. Wollenberger, W.Stöcklein, and F.W. Scheller, Electrochim. Acta 53 (2007) 1127.
[14] S.Y. Song, and H.C. Yoon, Sens. Actuators B Chem. 140 (2009) 233.
[15] S.Y. Song, Y.D. Han, Y.M. Park, C.Y. Jeong, Y.J. Yang, M.S. Kim, Y. Ku, and H.C. Yoon, Biosens. Bioelectron. 35 (2012) 355.
[16] D.M. Kim, and Y.B. Shim, Anal. Chem. 85 (2013) 6536.

[17] J.M. Moon, D.M. Kim, M.H. Kim, J.Y. Han, D.K. Jung, and Y.B. Shim, Biosens. Bioelectron. 91 (2017)128.
[18] G. Liu, S.M. Khor, S.G. Iyengar, and J.J. Gooding, Analyst 137 (2012) 829.
[19] K. Ogawa, D. Stöllner, F. Scheller, A. Warsinke, F. Ishimura, W. Tsugawa, S. Ferri, and K. Sode, Anal. Bioanal. Chem. 373 (2002) 211.
[20] S. Ferri, and K. Sode, Electrochemistry 80 (2012) 293.
[21] U. Jain, S. Gupta, and N. Chauhan, International Journal of Biological Macromolecules 105 (2017) 549.
[22] T. Kong, Y. Chen, Y. Ye, K. Zhang, Z. Wang, and X. Wang, Sens. Actuators B 138 (2009) 344.
[23] X. Liu, Q. Hu, Q. Wu, W. Zhang, Z. Fang, and Q. Xie, Colloids, and Surfaces B: Biointerfaces 74 (2009) 154.
[24] M.H. Asif, S.M.U. Ali, O. Nur, M. Willander, C. Brännmark, P. Strålfors, U.H. Englund, F. Elinder, and B. Danielsson, Biosens. Bioelectron. 25 (2010) 2205.
[25] R. Ahmad, N. Tripathy, J.H. Kim, and Y.B. Hahn, Sens. Actuators B 174 (2012) 195.
[26] J.Y. Kim, S. Jo, G. Sun, A. Katoch, S. Choi, and S.S. Kim, Sens. Actuators B 192 (2014) 216.
[27] B.N. Aini, S. Siddiquee, K. Ampon, K.F. Rodrigues, and S. Suryani, Sensing and Bio-Sensing Research 4 (2015) 46.
[28] H.A. Wahab, I.K. Battisha, A.A. El Saeid, and A.A. Salama, Results in Physics 9 (2018) 809.
[29] S. Chaudhary, A. Umar, K.K. Bhasin, and S. Baskoutas, Materials 11 (2018) 287.
[30] R. Arvizo, R. Bhattacharya, and P. Mukherjee, Expert opinion on drug delivery 6 (2010) 753.
[31] K.H. Liao, Y.S. Lin, C.W. Macosko, and C.L. Haynes, ACS Appl. Mater. Interfaces 7 (2011) 2607.
[32] S. Chawla, Anal. Biochem. 430 (2012) 156.
[33] Y. Huang, and H. Qiu, Vacuum 71 (2003) 523.
[34] B. Liu, and H.C. Zeng, J. Am. Chem. Soc. 125 (2003) 4430.
[35] S.M. Mahpeykar, J. Koohsorkhi, and H. GhafooriFard, Nanotechnology 23 (2012) 16560.
[36] M.K. Tabatabaei, H.G. Fard, and J. Koohsorkhi, Nano 10 (2015) 1550040.
[37] M.M.H. Shahkarami, J. Koohsorkhi, and H.G. Fard, Nano 12 (2017) 1750044.
[38] S. Karthik, P. Siva, K.S. Balu, R. Suriyaprabha, V. Rajendran, and M. Maaza, Advanced Powder Technology 28 (2017) 3184.
[39] H.G. Fard, J. Koohsorkhi, J. Mohammadnejad Arough, IET nanobiotechnology 14 (2020) 126.
[40] D. Basu, and R. Kulkarni, Indian J. Anaesthesia 58 (2014) 529.

[41] A. Mattewal, S. Aldasouqi, and D. Solomon, J. Diabetes Sci. Technol. 1 (2007) 879.
[42] S. Chawla, and C.S. Pundir, Anal. Biochem. 430 (2012) 156.
[43] Y. Zhou, H. Dong, L. Liu, Y. Hao, Z. Chang, M. Xu, Biosens. Bioelectron. 64 (2015) 442.